

# Separated Flows Around Spoilers and Forward-Facing Flaps

W. W. H. Yeung\* and C. Xu†

*Nanyang Technological University, Singapore 639798*

This paper presents experimental studies on the wall pressure and sectional force induced by the flows around a spoiler and a forward-facing flap mounted on a flat surface under various situations. When the spoiler and flap are stationary, the  $C_p$  distributions are similar because the flows are associated with an upstream zone where the pressure builds up gradually and a recirculating region downstream in which  $C_p < 0$ . The latter is bound by a shear layer from the spoiler/flap tip and a reattachment point on the surface, and its extent is dependent upon the spoiler/flap inclination. Base venting changes the flow structures by creating another shear layer from the additional tip so that the recirculating region becomes a wake. The resulting wall pressure and the overall sectional force components are found to vary appreciably with the gap size. When a nonvented spoiler undergoes a rapid rotation, a nonlinear pressure variation caused by a strong starting vortex shed from the spoiler tip is recorded downstream. The nonlinearity is found to decrease with increasing base-venting because of a counter-rotating starting vortex shed from the lower tip of the spoiler, as confirmed by flow visualization. However, when a forward-facing flap with or without base-venting undergoes such a rapid motion, a relatively weak vortical flow is found such that the pressure induced is more monotonic, as well as the sectional force. Hence, the studies indicate that the use of forward-facing flaps may have smaller transient adverse effects if mounted on airfoils.

## Nomenclature

$C_f$	= sectional force coefficient
$C_{fd}$	= sectional force coefficient downstream of model
$C_{fu}$	= sectional force coefficient upstream of model
$C_p$	= pressure coefficient, $2(p - p_\infty)/\rho U^2$
$c$	= airfoil chord
$g$	= gap size of model, i.e., spoiler or forward-facing flap
$H$	= height of wind-tunnel test section
$h$	= model height
$L$	= length of wind-tunnel test section
$p$	= static pressure on tunnel floor
$p_s$	= freestream static pressure
$Re$	= Reynolds number
$t$	= time
$U$	= freestream speed
$W$	= width of wind-tunnel test section
$x$	= streamwise distance
$x_0$	= streamwise location of model
$\alpha$	= angle of attack of airfoil
$\Gamma$	= strength of starting vortex
$\delta$	= boundary-layer thickness
$\theta$	= inclination of model
$\rho$	= density of air
$\omega$	= angular speed of model

## Introduction

A SPOILER is usually deployed rapidly during aircraft landing to reduce the lift and increase the drag. However, in addition to having a considerable time lag, the solid-type spoiler also induces an initial increase in lift<sup>1,2</sup> and decrease in moment<sup>2</sup> before reaching its long-term values. These adverse phenomena are attributed to the vortical flow of a strong starting vortex shed from the spoiler tip.<sup>2</sup> Investigating the unsteady flow behind the spoiler, particularly the transient pres-

sure development, provides an understanding of the associated flow nature and eventually helps identify means of reducing the adverse effects.

Experimental studies of various aspects of the unsteady flow developed behind a rapidly deployed spoiler have been reported in the literature. For example, the convection speed of the starting vortex shed from the spoiler tip was estimated by examining the variations of surface pressure induced by a floor-mounted spoiler undergoing a rapid rotation, e.g., 45 deg in 0.005 s (Ref. 3). By using flow visualization together with surface pressure and hot-wire measurements, the frequency range for the production of large coherent vortices of a lifting-spoiler flow was investigated.<sup>4</sup> The pressure response behind the spoiler mounted on a supercritical wing at a freestream Mach number of 0.2 was found to be nonlinear during a ramp-type motion of the spoiler.<sup>5</sup> This nonlinear variation, which appeared mainly on the rear part of the airfoil upper surface, was closely linked to the adverse behaviors in lift and moment. More recently, detail measurements of the flowfield by a laser Doppler anemometer and surface pressure developments behind a spoiler in either oscillating or pitch-and-hold motion confirmed that the vorticity transport was convective.<sup>6</sup> Measurements of the flow, such as wall pressure data together with prescribed criteria for the detection of flow reversal, were used to identify the onset of separation and reattachment of the unsteady flow of a moving flap.<sup>7</sup> Even though the adverse phenomena have been known for some time,<sup>1</sup> work on reducing the effects is rather limited. Recently, spoilers with base-venting, which is defined as the shortest distance (or gap size  $g$ ) between the lower tip of the spoiler deflected at  $\theta = 90$  deg and the neighboring airfoil surface, have shown to be a possible means of reducing the adverse lift and moment by their direct measurements.<sup>8</sup> However, pressure measurements and flow visualization of rapidly moving base-vented spoilers have yet to be reported in the literature. The results of the investigation reported here are on comparing the flows around a spoiler and a forward-facing flap<sup>9</sup> in terms of the induced pressure and sectional force, which are closely related to the adverse effects.

This paper contrasts the flows around a stationary spoiler and a forward-facing flap mounted on a wind-tunnel floor by examining the corresponding wall pressure and force variations. Base-venting is found to change the flow structures

Received April 13, 1997; revision received July 25, 1997; accepted for publication July 28, 1997. Copyright © 1997 by the American Institute of Aeronautics and Astronautics, Inc. All rights reserved.

\*Lecturer, School of Mechanical and Production Engineering.

†Graduate Student, School of Mechanical and Production Engineering.

downstream from a recirculating zone to a wake, and it influences the pressure and force of the flat wall in close proximity. The transient pressure and force developments behind a rapidly deployed spoiler and flap are then compared. The nonlinear pressure variation behind a spoiler is caused by the strong starting vortex. The pair of counter-rotating vortices behind a base-vented spoiler observed in flow visualization and the diminishing nonlinearity in pressure with increasing gap size indicate why the adverse effects may be reduced with base-venting.<sup>8</sup> The more monotonic pressure and force variations found behind a flap undergoing a rapid rotation with or without base-venting suggest that if there is any adverse effect caused by the forward-facing flap on an airfoil, it will be comparatively weaker than that caused by the spoiler.

### Experimental Setup

All tests were performed in an open-circuit wind tunnel with a 200 mm  $H \times 200$  mm  $W \times 700$  mm  $L$  working section. Five models used as spoilers as well as forward-facing flaps were machined from aluminium flat plates, all having a fixed height  $h = 10$  mm, but with five different gap sizes for base-venting, i.e.,  $g/h = 0, 0.5, 1.0, 1.5$ , and  $2.0$ . The blockage effect on pressure may be significant so that the blockage ratio  $h/H$  is kept as low as 5% at  $\theta = 90$  deg. Each plate spans the test section and has both upper and lower edges chamfered. When retracted, each model can be flush mounted on the tunnel floor, which is installed with pressure taps along the centerline, as shown schematically in Fig. 1. The rotation of a spoiler having its base at  $x_0/h = 11.5$  measured from the tunnel entrance is carried out by a simple mechanism mounted on a side wall. This mechanism consists of a pneumatic cylinder with its stroke connected to a variable resistor for the indication of the time of actuation. By mounting the mechanism on the other side wall, the setup can be used for tests involving a forward-facing flap of which the rotation is opposite to that of a spoiler.

The tunnel speed for all tests is kept at approximately  $U = 10$  m/s so that  $Re$  based on spoiler height is about  $6.45 \times 10^3$ , and  $\delta$  at the test position is about  $0.4h$ . The transient surface pressure during the rapid deployment of the model is measured at 15 locations in front of and behind the model by 15 Sensym SCXL004 differential pressure transducers with amplifiers. Data logging of the pressure and voltage across the variable resistor is carried out by a custom-made program controlling an AX5412 data-acquisition board of a maximum sampling rate of 90 kHz installed inside a personal computer. The power supplies to the transducers and the variable resistor are from two 6 V dc batteries that are separate to avoid interference from using any ac power source as detected in earlier tests. To keep the distortion of pressure signals to a minimum,<sup>10</sup> the tubing used had an i.d. of 1.35 mm and a length of about 2 cm between a transducer and a tap. An internal volume of less than  $0.1 \text{ cm}^3$  exists in each transducer. From the study of the

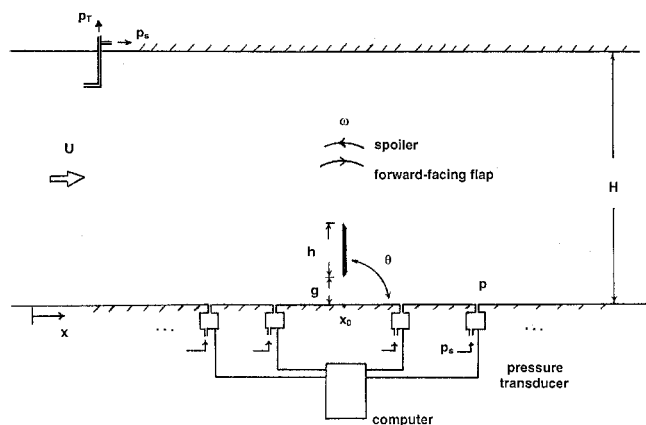


Fig. 1 Experimental setup.

overall frequency response of each transducer, a slight resonance is observed at about 60 Hz with an amplification factor of 1.1. The equipment is adequate for the present study because the pressure is induced by large vortical structures that are encountered. The maximum uncertainty of the pressure measurements is estimated to be 10%. A pitot static tube is placed near the tunnel entrance to provide the reference and dynamic pressures that are not affected by the transient motion of the model. A Nicolet 310 oscilloscope with two input channels is used to monitor the variations of one pressure port and the voltage across the variable resistor during the actuation of the spoiler or flap. The pressure data are integrated numerically by using MATLAB software.

### Stationary Spoilers and Forward-Facing Flaps

The flow around a stationary nonvented spoiler ( $g/h = 0$ ,  $0 < \theta \leq 90$  deg) mounted on a plane surface is characterized by an upstream region of gradual rise in pressure, where  $C_p > 0$ , and a downstream region of rising pressure, but with  $C_p < 0$ , as shown in Fig. 2a. An upstream separation bubble is often found near the front base of the spoiler as a result of flow deceleration leading to boundary-layer separation. A recirculating zone, which is bound by the shear layer emanating from the spoiler tip and terminated at a reattachment point on the flat surface, is the flow nature behind the spoiler. The extents of the bubble and the recirculating zone depend on the Reynolds number. While the recirculating zone is easily detected by pressure measurements, the bubble that is generally smaller in size is best observed by using flow visualization. The preceding qualitative comparison between the flows around spoilers and flaps, which may be obvious, indicates that should the spoiler be replaced by the flap, no undesirable steady effect will be introduced.

Table 1 summarizes the pertinent flow parameters. In Fig. 3a, static pressure distributions on a plane surface fitted with a stationary flat plate ( $\theta = 90$  deg) in a uniform upstream flow<sup>11,12</sup> are presented for comparison. Close agreement is found between the reported data<sup>11</sup> and the present measurements. However, because of the large blockage effect, the  $C_p$  values<sup>12</sup> downstream of the spoiler are found to be more negative. The pressure rise upstream and the extent of suction downstream of the spoiler both increase with the inclination, as depicted in Fig. 4a for  $\theta = 30, 60$ , and  $90$  deg.

While a spoiler has its tip facing downstream of the main flow, the tip of a forward-facing flap points against it, if  $90 \text{ deg} < \theta < 180 \text{ deg}$  (Fig. 2b). With the help of boundary-layer control, a forward-facing flap mounted above a wing was originally designed to establish a flow about a very thick pseudo-wing to provide good low-speed properties. When the flap is mounted on a flat surface in the absence of boundary-layer control, the approaching flow on one hand stagnates somewhere in front of the flap, forming a separation bubble underneath the stagnation point, and on the other hand separates at the tip to form a shear layer, giving rise to a flow very similar in nature to that of a spoiler, i.e.,  $C_p > 0$  for  $x < x_0$  and  $C_p < 0$  for  $x > x_0$ , as indicated in Fig. 5a for  $\theta = 90, 120$ , and  $150$  deg. In comparison with Fig. 4a, the flap inclination does not

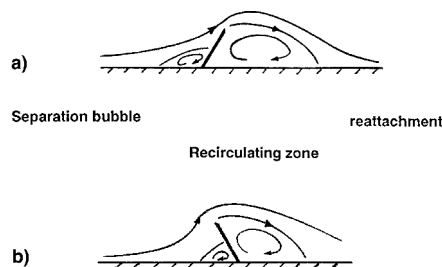
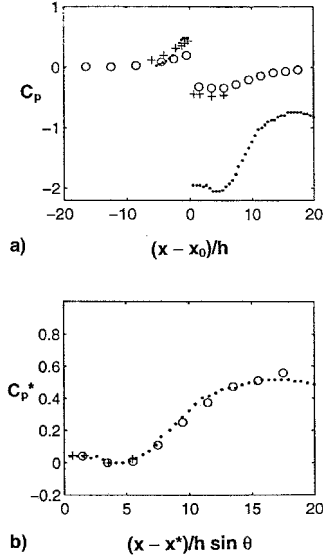
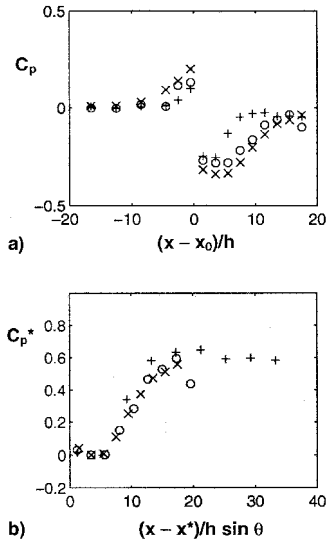


Fig. 2 Flow around floor-mounted a) spoiler and b) forward-facing flap.

**Table 1** Comparison of flow parameters

Parameter	References		Present
	11	12	
$Re$	3500	2600	6450
$\delta/h$	0.72	0.34	0.4
$b/H$	1.5%	21%	5%

**Fig. 3** Wall pressure induced by stationary flat plate ( $g/h = 0$ ,  $\theta = 90$  deg) (+, Ref. 11; \*, Ref. 12; o, present study).**Fig. 4** Wall pressure induced by stationary spoiler ( $g/h = 0$ ) (+,  $\theta = 30$  deg; o,  $\theta = 60$  deg; x,  $\theta = 90$  deg).

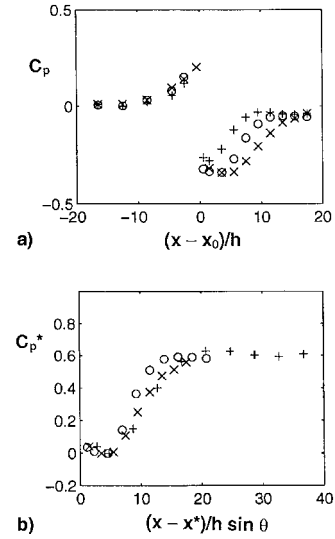
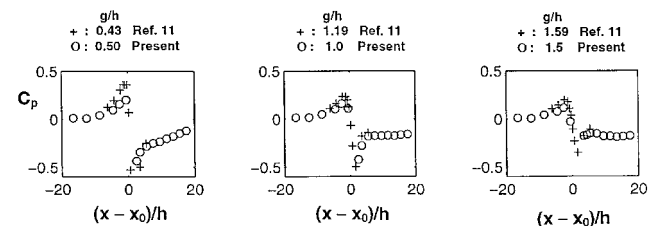
affect the pressure gradient upstream significantly, but the extent of suction behind the flap is found to decrease with increasing  $\theta$ .

Separated reattaching flows have similar pressure distributions and they can often be collapsed onto a universal curve when plotting a modified pressure coefficient with respect to a relevant length scale, such as the reattachment length.<sup>13</sup> The data in Figs. 3a, 4a, and 5a, when converted to the modified pressure coefficient

$$C_p^* = \frac{C_p - \min(C_p)}{\max(C_p) - \min(C_p)}$$

and plotted against  $(x - x^*)/h \sin \theta$ , where  $x^* = x_0 + h \cos \theta$  is the streamwise location of the spoiler/flap tip, are found to collapse onto a universal curve shown in Figs. 3b, 4b, and 5b, indicating that the basic trend of  $C_p$  in the recirculating region is independent of the Reynolds number, boundary-layer thickness, blockage, and inclination, and that the streamwise location of the spoiler/flap tip is a basic length scale here. Note that  $\max(C_p)$  and  $\min(C_p)$  come from the corresponding set of  $C_p$  measurements. The seven sets of data were originally plotted on one graph and a good collapse of data was found. However, the plot is not chosen for presentation because the data points are too close to be identified clearly.

If base-venting is introduced, another shear layer is formed at the lower tip of the spoiler/flap. The separation bubble upstream may be eliminated by the flow through the gap to allow for a more gradual pressure rise. The recirculating region is replaced by a wake enclosed by the two shear layers and possibly the flat surface downstream, depending on the gap size. Reasonably good agreement is found in Fig. 6 between the measurements<sup>11</sup> at  $g/h = 0.43$ , 1.19, and 1.59, and the present data where  $g/h = 0.5$ , 1.0, and 1.5. Vortex shedding detected at  $g/h \geq 0.55$  (Ref. 11) may explain why the transient surface pressure at  $0 < (x - x_0)/h \sin \theta < 20$  exhibits considerably large fluctuations when  $g/h > 0.5$ , as found in the present study (not shown). As indicated in Fig. 7, where  $g/h = 0.5$ , 1.0, 1.5, and 2.0 and  $\theta = 60$ , 90, and 120 deg, the effect of base-venting is reflected by a more gradual rise in pressure upstream to attain a lower maximum when the gap size is increased. Although the pressure downstream of the gap is found to recover sharply with  $g/h \geq 1$ , it is strongly affected by the lower shear layer and remains negative for a long distance. For instance,  $C_p = -0.15$  within  $5 < (x - x_0)/h \sin \theta < 20$  for  $g/h = 1.0$  and  $\theta = 60$ , 90, and 120 deg. The extent of constant pressure increases more steadily with inclination than with gap size, sug-

**Fig. 5** Wall pressure induced by stationary forward-facing flap ( $g/h = 0$ ) (x,  $\theta = 90$  deg; o,  $\theta = 120$  deg; +,  $\theta = 150$  deg).**Fig. 6** Wall pressure induced by stationary base-vented flat plate ( $\theta = 90$  deg).

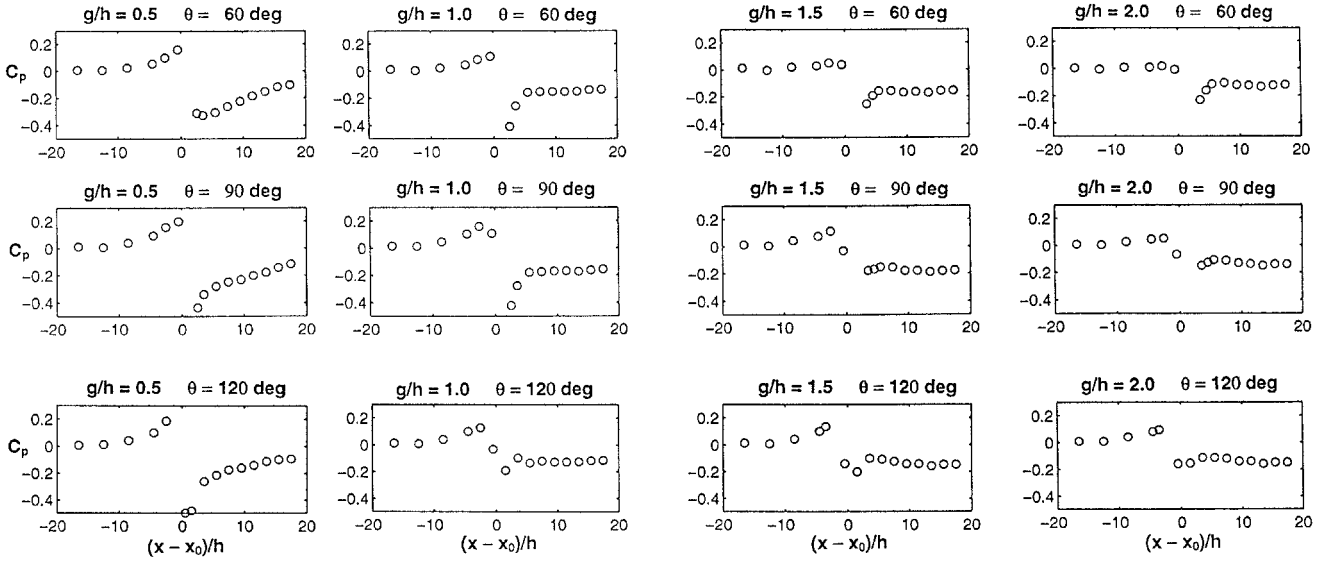


Fig. 7 Wall pressure induced by stationary base-vented spoiler and flap.

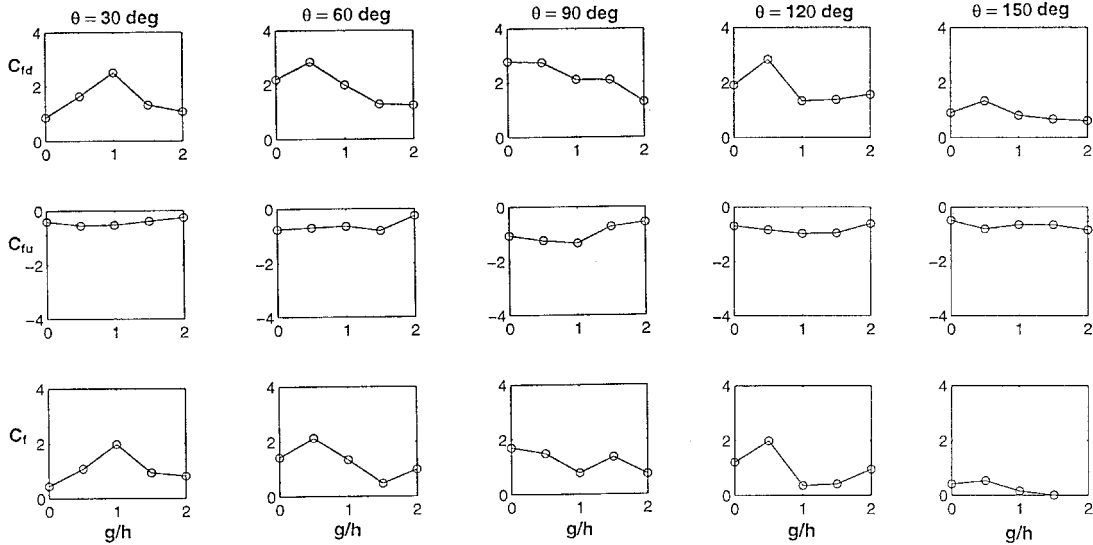


Fig. 8 Variations of normal force components with gap size.

gesting that the lower shear layer from the flap may tug away from the flat surface earlier than that of the spoiler.

The sectional normal forces acting on the flat surface upstream and downstream of the spoiler/flap can be obtained by integrating the corresponding pressure distributions; that is,

$$C_{fu} = \int_0^{-\infty} (-C_p) d \frac{(x - x_0)}{h}, \quad C_{fd} = \int_0^{\infty} (-C_p) d \frac{(x - x_0)}{h}$$

The variations of  $C_{fu}$ ,  $C_{fd}$ , and their sum  $C_f$  with respect to the gap size, are given in Fig. 8. The following points are noteworthy.

1)  $C_{fd} > 0$  and  $C_{fu} < 0$  for all values of  $\theta$  and  $g/h$ . In other words, suction is found behind the spoiler/flap to give rise to an upward force, whereas pressure is in front to induce a downward force.

2) For most cases (except  $\theta = 150$  deg), the magnitudes of  $C_{fd}$  are larger than those of  $C_{fu}$ . Therefore, a net positive  $C_f$  results.

3) While  $C_{fd}$  decreases monotonically with the gap size at  $\theta = 90$  deg, it increases in  $0 < g/h < 0.5$ , and decreases thereafter for  $\theta = 60, 120$ , and  $150$  deg. For  $\theta = 30$  deg, the range of increasing  $C_{fd}$  is enlarged to  $0 < g/h < 1$ . The attenuation of

$C_{fd}$  at large values of  $g/h$  reflects that the influence from spoiler/flap diminishes with increasing base-venting. The extent of suction region at  $g/h = 0.5$  is larger than that at  $g/h = 0$  for all values of  $\theta$ , explaining why  $C_{fd}$  increases there.

4) The variation of  $C_{fu}$  with  $g/h$  is more gradual than that of  $C_{fd}$ , indicating that the change in flow structure takes place more dominantly behind the spoiler/flap.

5) The values as well as the variation of  $C_{fd}$  with respect to  $g/h$  at  $\theta = 60$  deg, i.e., spoiler, are almost identical to those at  $\theta = 120$  deg, i.e., forward-facing flap. However, they are drastically different at  $\theta = 30$  and  $150$  deg, perhaps because of the orientation of the lower shear layer.

The fact that  $C_p^*$  and  $(x - x^*)/h \sin \theta$ , where  $x^* = x_0 + g \cos \theta$ , or  $x_0 + (g + h) \cos \theta$ , fail to collapse the pressure data at various gap sizes and inclinations to a universal curve, strongly suggests that the nature of the flow structure is different from the nonvented case.

### Rapidly Deployed Spoiler

When a nonvented spoiler undergoes an angular rotation from 0 to 90 deg at  $\omega = 6923$  deg/s or  $\omega h/U = 0.12$ , the  $C_p$  variations along the tunnel floor at nine instants as marked in Fig. 9a for the angular variation are depicted sequentially in

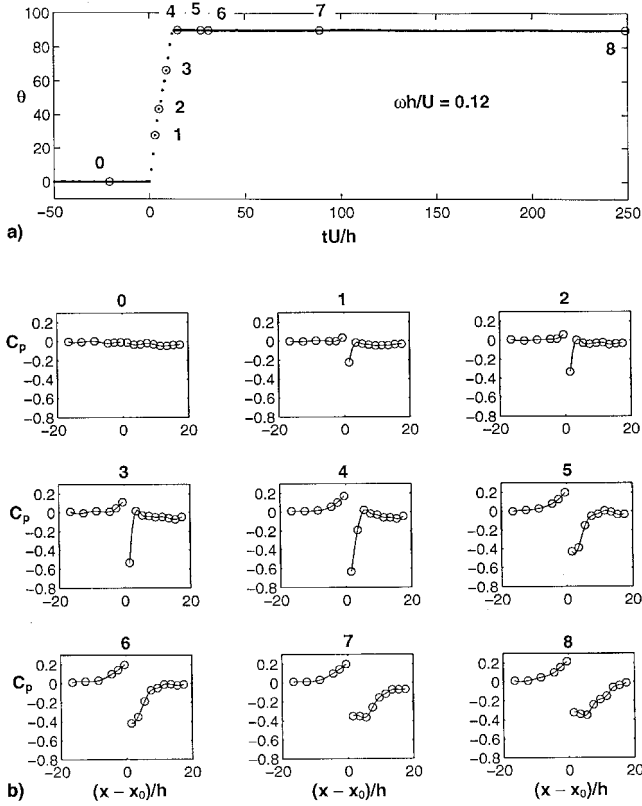


Fig. 9 Transient wall pressure induced by moving spoiler ( $g/h = 0$ ,  $\theta = 0 \rightarrow 90$  deg).

Fig. 9b. Pressure in front of the spoiler rises monotonically at all times, whereas suction is found behind the spoiler such that it overshoots the steady-state value at some instants. This non-linear variation is attributed to the roll-up and convection of the starting vortex behind a rapidly deployed spoiler, as clearly indicated in the flow-visualization pictures<sup>7</sup> and flowfield measurements.<sup>6</sup> At a fixed location downstream of the spoiler, e.g.,  $1 < (x - x_0)/h < 5$  (Refs. 6 and 7), the surface pressure induced by this convective vortex increases slightly from its initial value and decreases sharply to attain a suction peak. It then recovers to reach another maximum before settling to its steady-state value associated with the steady separated flow, similar to the transient pressure variation shown in Fig. 10a, measured at  $(x - x_0)/h = 1.5$  or  $(x - x^*)/h = 0.5$ , although the initial increase is not obvious here. The case where  $\omega h/U > 1$  is not included because of the limitations of the equipment in achieving larger values of  $\omega$  or recording pressure signals at  $U \approx 1$  m/s.

When a base-vented spoiler is deployed in the direction opposite to the mainstream, strong shear flows at its tips produce a pair of counter-rotating vortices. Figure 11 shows a sequence of typical photographs of flow visualization obtained by using smoke and captured by a video camera, confirming the formation and convection of this vortex pair behind a spoiler ( $g/c = 5\%$ ) undergoing a rapid rotation about 500 deg/s on the upper surface of an airfoil at  $\alpha = 0$  deg. The spoiler, which has a height of 10%, is pivoted at 70% chordwise position, and  $Re = 2.15 \times 10^3$ , based on the spoiler height.

Because the vortex shed from the lower tip of the spoiler has the opposite sense of rotation to the vortex shed from the upper tip, the net circulation behind the spoiler is thus reduced. As a result, the induced suction peak in Fig. 10a diminishes as the gap size increases, as depicted in Figs. 10b–10e, recorded at  $(x - x^*)/h = 0.5$  for  $g/h = 0.5, 1.0, 1.5$ , and 2.0, respectively, with the suction peak decreasing from  $-0.64$  to  $-0.35$ . The reductions in adverse lift and moment<sup>8</sup> brought about by base-venting are closely related to the corresponding

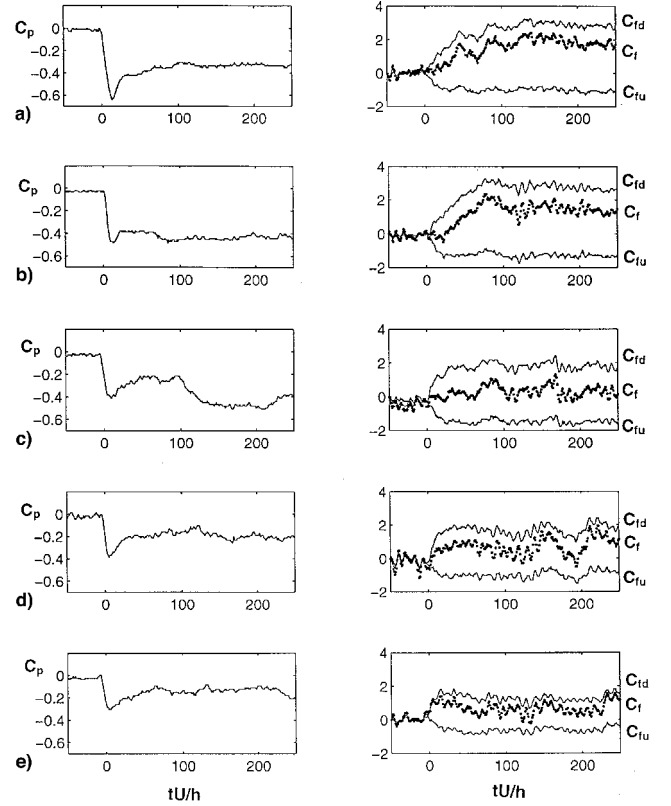


Fig. 10 Comparisons of transient wall pressure at  $(x - x^*)/h = 0.5$  and overall force components induced by base-vented moving spoiler ( $\theta = 0 \rightarrow 90$  deg).  $g/h =$  a) 0, b) 0.5, c) 1.0, d) 1.5, and e) 2.0.

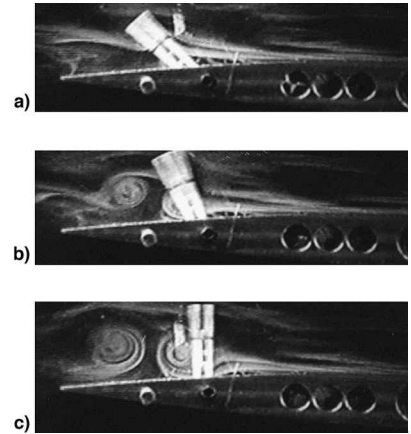


Fig. 11 Flow visualization of vortices behind base-vented spoiler on airfoil ( $g/c = 5\%$ ,  $\alpha = 0$  deg,  $\omega = 500$  deg/s).

reduction in this suction peak. Large fluctuations after the suction peak are found in Figs. 10c–10e, suggesting that vortex shedding may take place in the wake when  $g/h > 0.55$ .<sup>11</sup> The developments of  $C_{fd}$ ,  $C_f$ , and  $C_{tu}$  at the various gap sizes given in Fig. 10 indicate that because of the relatively strong vortical flow behind the spoiler, the durations taken for  $C_{fd}$  and  $C_f$  to reach their steady values are longer for  $g/h = 0$  and 0.5 than for  $g/h = 1.0, 1.5$ , and 2.0, and that larger fluctuations in  $C_{fd}$  and  $C_f$  are observed at  $g/h = 0$  and 0.5.

### Rapidly Deployed Forward-Facing Flap

Because of the orientation of a forward-facing flap, its tip moves in the same direction as the oncoming flow when the flap is deployed rapidly. If the speed of the flap tip is smaller than the neighboring fluid speed, such as the case elucidated

in Fig. 12a, a starting vortex of clockwise rotation in sense is formed by the shear flow near the flap tip. However, the strength of this starting vortex, which depends on the velocity gradient at the tip, is weaker than the one associated with the spoiler tip moving against the oncoming flow. If, on the other hand, the tip speed of the flap is much larger than the neighboring fluid speed, the starting vortex formed is initially anti-clockwise and eventually dispersed in the shear flow downstream of the tip (Fig. 12b). Figure 13b depicts the sequential  $C_p$  variations along the tunnel floor that are induced by a non-vented flap undergoing an angular rotation from 0 to 90 deg at  $\omega = 6923$  deg/s or  $\omega h/U = 0.12$ , i.e., the case in Fig. 12a, at nine instants (Fig. 13a). The more gradual pressure drop downstream of the flap in Fig. 13 as compared to that of the spoiler in Fig. 9 is the result of the weaker rotational flow associated with a rapidly deployed forward-facing flap. As shown in Fig. 14a, which is recorded at  $(x - x_0)/h = 1.5$  or  $(x - x^*)/h = 2.5$  with  $\theta = 180$  deg  $\rightarrow$  90 deg at  $\omega = 6923$

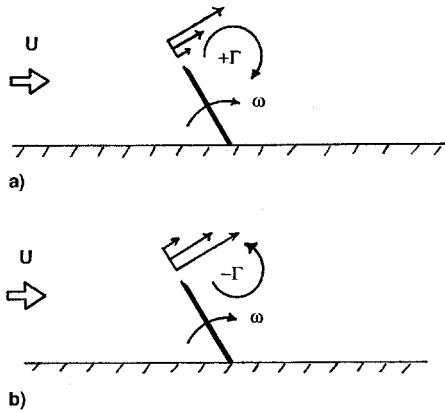


Fig. 12 Starting vortex behind forward-facing flap: a)  $U > \omega h$  and b)  $U < \omega h$ .

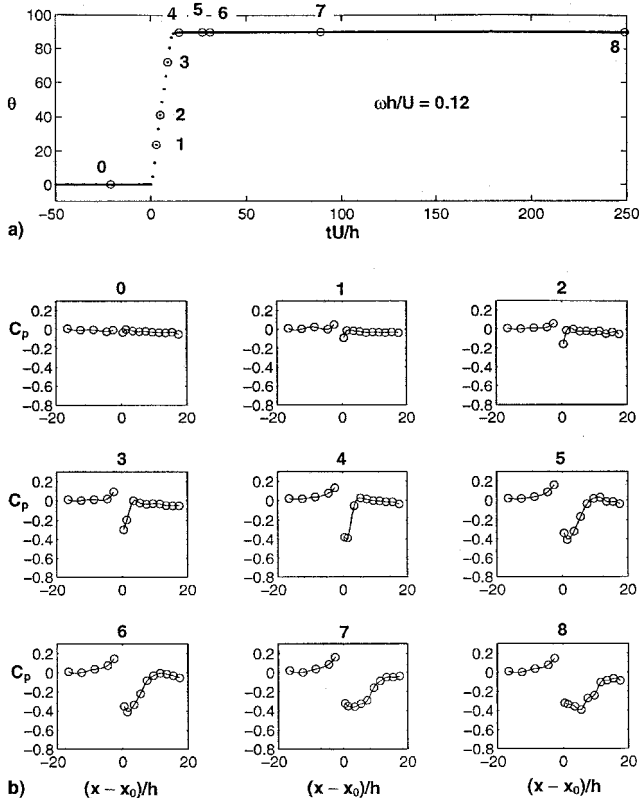


Fig. 13 Transient wall pressure induced by moving forward-facing flap ( $g/h = 0$ ,  $\theta = 180$  deg  $\rightarrow$  90 deg).

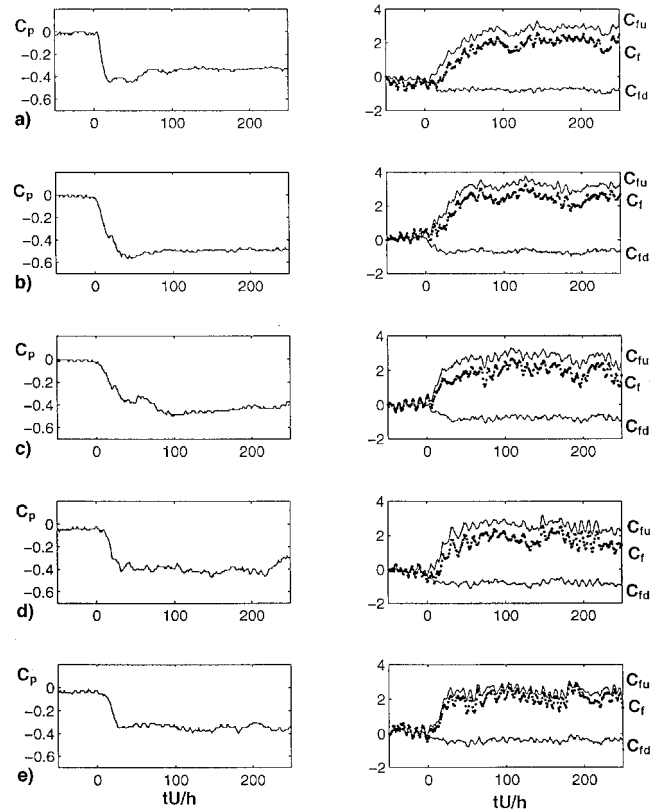


Fig. 14 Comparisons of transient wall pressure at  $(x - x^*)/h = 0.5$  and overall force components induced by base-vented moving forward-facing flap ( $\theta = 180$  deg  $\rightarrow$  90 deg).  $g/h =$  a) 0, b) 0.5, c) 1.0, d) 1.5, and e) 2.0.

deg/s, the pressure is found to drop monotonically with a weaker starting vortex rather than having an obvious overshoot (Fig. 10a). Therefore, the adverse effects caused by a rapidly deployed flap, if any, are less significant than those by the spoiler. And when base-venting is introduced, transient pressure measurements corresponding to  $g/h = 0.5$ , 1.0, 1.5, and 2.0 at  $(x - x^*)/h = 2.5$  with  $\theta = 180$  deg  $\rightarrow$  90 deg and the same  $\omega$ , as shown in Figs. 14b–14e, all have a monotonic decrease of pressure. Although the time taken for  $C_f$  to reach its steady value is longer for  $g/h = 0$  and 0.5 than for  $g/h = 1.0$ , 1.5, and 2.0, smaller fluctuations in  $C_f$  are observed at all values in  $g/h$  as compared to Fig. 10, suggesting that base-venting does not introduce any adverse effect.

## Conclusions

From the wall pressure measurements and the integrated sectional force, the basic flow structure associated with a stationary nonvented spoiler is similar to that with a forward-facing flap, both having a strong recirculating region with  $C_p < 0$ , although its extent depends on the inclination. Base-venting changes the previously mentioned recirculating region to a wake because of the shear layer from the lower tip. The orientation of this lower shear layer may influence the downstream wall pressure and the induced normal force. If the gap size is large, the upper and lower shear layers may interact to create vortex shedding. The wall pressure may exhibit large fluctuations, and the normal force is reduced.

When a nonvented spoiler is deployed rapidly, a starting vortex is shed from the tip and convects downstream, accounting for the nonlinear pressure induced. Flow visualization demonstrates that a pair of counter-rotating transient vortices is shed behind the spoiler. Because of the reduction in circulation, the nonlinear variation of the induced wall pressure is reduced, explaining why base-venting abates the transient adverse lift and moment of spoilers. The time taken for the nor-

mal force to reach its steady-state value decreases with increasing gap size.

During the rapid deployment of a forward-facing flap (with or without base-venting), the wall pressure downstream is found to decrease monotonically without any overshoot in suction, as detected in the case of spoilers. The fluctuations in the normal force are small compared to the rapidly deployed spoiler. Because the flows around a stationary spoiler and a forward-facing flap are similar, the forward-facing flap at rapid deployment may be used to replace the spoiler for the purpose of reducing the transient adverse effects.

### Acknowledgment

The authors thank Z. K. Ng for assistance with the experimental setup and measurements.

### References

- <sup>1</sup>Hoerner, S. F., and Borst, H. V., *Fluid-Dynamic Lift*, 2nd ed., Hoerner Fluid Dynamics, Albuquerque, NM, 1985.
- <sup>2</sup>Mabey, D. G., "A Review of Some Recent Research on Time-Dependent Aerodynamics," *Aeronautical Journal*, No. 1099, Feb. 1984, pp. 23–37.
- <sup>3</sup>Ahmed, S., and Hancock, G. J., "On the Local Flow About a Spoiler Undergoing Transient Motion at Subsonic Speeds," Queen Mary College, QMC/EP-1050, London, June 1983.
- <sup>4</sup>Reisenthel, P. H., Nagib, H. M., and Koga, D. J., "Control of Separated Flows Using Forced Unsteadiness," AIAA Paper 85-0531, March 1985.
- <sup>5</sup>Costes, M., Gravelle, A., Philippe, J. J., Vogel, S., and Triebstein, H., "Investigation of Unsteady Subsonic Spoiler and Flap Aerodynamics," *Journal of Aircraft*, Vol. 24, No. 9, 1987, pp. 629–637.
- <sup>6</sup>Nelson, C. F., Koga, D. J., and Eaton, J. K., "Unsteady, Separated Flow Behind an Oscillating Two-Dimensional Spoiler," *AIAA Journal*, Vol. 28, No. 5, 1990, pp. 845–852.
- <sup>7</sup>Ramiz, M. A., and Acharya, M., "Detection of Flow State in an Unsteady Separating Flow," *AIAA Journal*, Vol. 30, No. 1, 1992, pp. 117–123.
- <sup>8</sup>Yeung, W. W. H., Xu, C., and Gu, W. D., "Reduction of Transient Adverse Effects of Spoilers," *Journal of Aircraft*, Vol. 34, No. 4, 1997, pp. 479–484.
- <sup>9</sup>Hurley, D., "The Use of Boundary Layer Control to Establish Free Streamline Flows," *Advances in Aeronautical Science*, Vol. 2, 1959, pp. 662–708.
- <sup>10</sup>Irwin, H. P. A. H., Cooper, K. R., and Girard, R., "Correction of Distortion Effects Caused by Tubing Systems in Measurements of Fluctuating Pressures," *Journal of Industrial Aerodynamics*, Vol. 5, 1979, pp. 93–107.
- <sup>11</sup>Everitt, K. W., "A Normal Flat Plate Close to a Large Plane Surface," *Aeronautical Quarterly*, 1982, pp. 90–104.
- <sup>12</sup>Kelso, R. M., Lim, T. T., and Perry, A. E., "The Effect of Forcing on the Time-Averaged Structure of the Flow Past a Surface-Mounted Bluff Plate," *Journal of Wind Engineering and Industrial Aerodynamics*, Vol. 49, 1993, pp. 217–226.
- <sup>13</sup>Roshko, A., and Lau, J. C., "Some Observations on Transition and Reattachment of a Free Shear Layer in Incompressible Flow," *Proceedings of the Heat Transfer and Fluid Mechanics Institute*, edited by A.F. Charwatt, Stanford Univ. Press, Stanford, CA, 1965, pp. 157–167.